Proceedings World Geothermal Congress 2005
Antalya, Turkey, 24-29 April 2005

Temperature and Compositional Changes in the Hydrothermal Fluids in the Mt. Amiata Geothermal Area: Evidence from Fluid Inclusion Data

Giovanni Ruggieri[1], Chiara Giolito[2], Giovanni Gianelli[1], Maria Luce Frezzotti[3]

[1]CNR – Institute of Geosciences and Earth Resources, Via Moruzzi 1, 56124 Pisa, Italy

[2]Department of Earth Sciences, University of Florence, Via La Pira 4, 50121 Florence, Italy

[3]Department of Earth Sciences, University of Siena, Via Laterina 8, 53100 Siena, Italy

ruggieri@igg.cnr.it, giolito@geo.unifi.it, gianelli@igg.cnr.it, frezzottiml@unisi.it

Keywords: Fluid inclusions, hydrothermal fluids, boiling, mixing, CO_2, Mt. Amiata geothermal field, Italy.

ABSTRACT

Two geothermal fields, Bagnore and Piancastagnaio, are in the southern sector of the Quaternary Amiata volcano (southern Tuscany, Italy). Fluid inclusions trapped in quartz, adularia and calcite found in core-sample in deep drilled wells (between 1690 and 3220 m below the ground level) of the geothermal fields provided information on the physical-chemical characteristics of circulating fluids in past. Three types of fluid inclusions related to the geothermal activity were recognized: type I (liquid-rich) inclusions trapped an aqueous fluid with CO_2 concentration (1.27-2.68 mol/kg) that is significantly higher than that of present-day fluids (0.11-0.05 mol/kg). Type II (liquid-rich) inclusions formed after type I, and trapped a fluid with lesser CO_2 (<0.85 mol/kg). Type III (vapor-rich) inclusions record an early fluid circulation under boiling conditions and in some samples coexist with type I inclusions. The decrease of CO_2 concentration from type I inclusions to type II inclusions, and then to present-day concentrations can be related to boiling with gas loss and/or mixing. In general type I and II inclusions show variable salinities (0.11-3.90 mol/kg of Na^+ and Cl^-) and Th (150-335°C), which can also be associated with boiling and mixing processes. In particular, the data suggest that mixing between a hot low-salinity fluid and a cooler saline fluid may has occurred in samples where present-day temperatures are in the range 195-280°C. On the other hand, the present-day hottest areas (295-320°C) appear to be nearly in thermal stability from the time of fluid inclusion trapping and mixing processes are not evident.

1. INTRODUCTION

Quantitative estimates of the physical-chemical conditions in active geothermal fields and their temporal and/or spatial variations are of great importance for an optimal exploitation of geothermal resources. Much of the information on geothermal reservoirs comes from direct in-hole measurements, core samples and geochemical data on the reservoir fluids.

Additional, and sometimes unique, information on the reservoir fluids can be obtained from studies of the fluid inclusions trapped within minerals formed during geothermal activity (Hedenquist et al., 1992; Cathelineau and Marignac, 1994). As fluid inclusions record the variation in the local fluid circulation conditions, they represent the fluids present in well-defined zones of the geothermal reservoir. They are, moreover, the only direct evidence of the paleo-fluids that have circulated at different times through the reservoir rocks. The study of fluid inclusions can, therefore, provide important information on the local characteristics of the reservoir and on the time-space evolution of its geothermal fluids.

Very little is known about the fluid inclusions of the Mt. Amiata geothermal field located in southern Tuscany (Italy) (Fig. 1). One sample from the Piancastagnaio area was studied for fluid inclusion data by Belkin et al. (1985), but no fluid inclusion data exist for the Bagnore area.

In this work we reconstruct some of the physical-chemical parameters of the hydrothermal fluids that circulated in the Mt. Amiata area, before present-day activity, from fluid inclusion data. We present the results of petrographic studies and microthermometric and Raman analyses on fluid inclusions trapped in minerals found in veins and breccias drilled in five wells of the Mt. Amiata geothermal field. By using temperature and compositional data of fluid inclusions and their comparison data with present-day values, we evaluate the changes that has occurred in the hydrothermal fluids and the processes responsible for such changes.

2. THE MT. AMIATA GEOTHERMAL FIELDS

In the late 1950s to early 1960s, two geothermal fields, Bagnore and Piancastagnaio, were discovered in the southern sector of the Quaternary Amiata volcano (Fig. 1). At that time the wells were producing from the shallow carbonate reservoir at depths of 500-1000 m below ground level (b.g.l.) (Bertini et al., 1995).

A second exploration programme, started in the 70s with a target at deeper reservoirs, revealed the presence of fractured layers at depths ranging from 1300 to 3000 m b.g.l. inside metamorphic units (Bertini et al., 1995). This reservoir is water-dominated, with a hydrostatic pressure of about 20-25 MPa, and temperatures around 300-350°C. The entire system is fed by a meteoric fluid circulating through fractures. The deep reservoir fluid is basically alkaline-chloride with high content of ammonium, boron and carbon dioxide (Bertini et al., 1995). The installed capacity in the Piancastagnaio and Bagnore fields is 91.5 and 20 MW, respectively (Cappetti et al., 2000).

The Amiata volcano (1770 m asl), which belongs to the Tuscan Magmatic Province, was active at 0.29-0.18 Ma, with volcanic products ranging in composition from trachydacitic to latitic (Ferrari et al., 1996).

The stratigraphic sequence in the Mt. Amiata area consists of the following units (from the top downward): 1) Mt. Amiata volcanic products (Quaternary); 2) marine sediments (Neogene); 3) flysch complexes belonging to the “Ligurid Units” (Cretaceous-Eocene); 4) calcareous-evaporitic and siliciclastic formations of the “Tuscan Nappe” (Upper Triassic); 5) metamorphic units: graphite phyllites, metasandstones inclusiong carbonate layers and chlorite phyllites with dolomitic intercalations (Paleozoic).

The geothermal system in the Mt. Amiata area appears to be related to, and dependent upon, a deep magmatic body, whose presence is indicated by fragments of two-mica granite and thermometamorphic minerals in cores (Gianelli et al., 1988).

The presence of a deep anomalous body is also suggested by geophysical data. Gravimetric data in this area show very low values despite the uplift of denser units, and imply the presence of a low density body at depth (Bernabini et al. 1995; Fiordelisi et al., 2000). Moreover, the seismic reflection data have revealed the presence of a zone in which there are no seismic reflection signals. The location and shape of the seismic-transparency zone show a similarity with the deep low-density body of the gravity anomaly, so that the zone has been interpreted as a batholith (Fiordelisi et al., 2000).

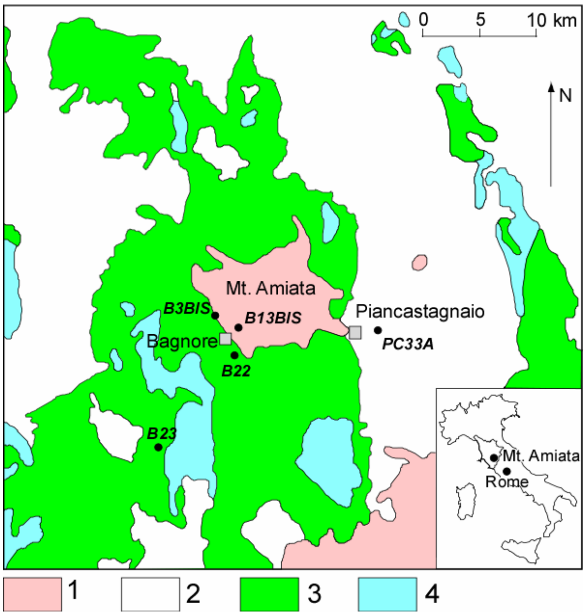

Figure 1: Geological sketch map of the Mt. Amiata geothermal field, showing the location of the two studied wells, modified after Bertini et al. (1995). 1) Volcanic products (Quaternary); 2) marine sediments (Neogene); 3) flysch complex of the “Ligurid Units” (Cretaceous-Eocene); 4) calcareous-evaporitic and siliciclastic formations of the “Tuscan Nappe” (Upper Triassic).

Geophysical investigations have revealed some peculiar features of the shallow structure in the Amiata area. Heat flow measurements have shown that a large thermal anomaly characterizes the volcano and in particular the areas of the Bagnore and Piancastagnaio geothermal fields, reaching values higher than 250 mW/m^2 (Baldi et al., 1995).

After stripping off the effects of volcanics and Neogene deposits, and of the large anomaly caused by the deep, low-density magmatic body, the gravity data still show residual lows in the Piancastagnaio area and further SW. These lows were interpreted as being caused by higher porosity and were modelled for depths of 100-800 m b.g.l. (Bernabini et al., 1995).

3. SAMPLES

Six core-samples have been selected for fluid inclusions analyses: B3BIS-2108, B3BIS-3111, B13BIS-3220, B22-2300 and B23-2036 (numbers after dash indicate the sampling depth in m b.g.l). These wells are located in the Bagnore area (Fig. 1), while the sample PC33A-1690 was from a well of the Piancastagnaio area (Fig. 1). At the sampling depths the wells crossed the Paleozoic metamorphic rocks (phyllites, chlorite phyllites with dolomitic intercalations layers).

3.1 Petrographic description

Two samples (B3BIS-3111 and B22-2300) are constituted by breccias of metamorphic rocks consisting of angular-to-sub-angular clasts of graphite phyllite, partially cemented by hydrothermal quartz, adularia, Mn-rich calcite (some with bladed habit), chlorite, illite, pyrite plagioclase (albite or oligoclase). In B3BIS sample, textural relationships indicate that the first deposited phase contains quartz, adularia and albite, which was followed by chlorite, illite and than calcite phases. In B22-2300 breccia quartz, adularia, albite and calcite are coeval, whereas illite and chlorite are a late phase.

The other samples (B3BIS-2108, B13BIS-3220, B23-2036 and PC33A-1690) are characterized by the presence of veins filled mostly by quartz or quartz and carbonates (dolomite-ankerite and/or siderite). A number of features, including veins folding, the widespread occurrence of quartz crystals with undulate extinctions and carbonates twining lamellae, indicate that most of these veins were undergone to stress and deformation. The formation of such veins may be, therefore, related to an event (Alpine?) of regional metamorphism, before the hydrothermal activity of the geothermal field.

Some of these samples, however, also evidenced the recent hydrothermal circulation related to geothermal activity. In particular, one samples (B13BIS-3220) is cross-cut by a late hydrothermal vein, made up of euhedral quartz crystals with normal extinction, calcite (with bladed habit), chlorite, illite and corrensite. Two other samples (B3BIS-2108 B23-2036) show that the metamorphic veins, were affected by the recent hydrothermal circulation that produce rare late euherdral quartz crystals with non-undulate extinctions in the central part of the veins.

4. FLUID INCLUSIONS

4.1 Methods

Microthermometric measurements were performed at the Institute of Geosciences and Earth Resources (IGG) of CNR (Pisa - Italy) using a Linkam THMSG 600 stage. The stage was calibrated by means of synthetic fluid inclusions containing H_2O with critical density and H_2O-CO_2 fluids. Reproducibility is in the order of ±0.1°C for temperatures below 40°C, and ±1.0°C for temperature >200°C.

Raman analyses of the gas phase of the fluid inclusions were performed at UMR CNRS G2R-7566 and CREGU (Nancy, France) using a DILOR X-Y multi-channel modular Raman spectrometer and at the Department of Earth Science of Siena University (Italy) using a LAB-RAMAN multi-channel spectrometer. Reproducibility of Raman analyses on the volatile components is within ± 1 mole %.

4.2 Fluid inclusion types, microthermometric and Raman data

The studied fluid inclusions are either hosted in hydrothermal minerals, mostly in quartz and more rarely calcite and adularia, occurring in veins and as breccia cement or in metamorphic quartz in veins. Final ice melting temperature (Tmi), clathrate melting temperature (Tmcl), CO_2 melting temperature ($TmCO_2$), CO_2 homogenisation temperature ($ThCO_2$) and total homogenisation temperature (Th) were systematically measured and the results are summarized in Tables 1, 2 and 3. In these Tables the present-day temperatures at the depth of sampling are also shown. Eutectic temperature (Te) could be measured only in few inclusions and these data are only described in the text.

Four types of fluid inclusions have been recognised on the basis of optical observations at room temperature, microthermometric data:

Type I inclusions are two-phase (liquid water + carbonic gas) liquid-rich inclusions which formed clathrates during freezing experiments. These inclusions occur in hydrothermal quartz in all samples, except B22-2300 and PC33A-1690. In some cases they occur as small, three-dimensional groups or along growth zones or as part of a random distribution throughout a single crystal. According to Roedder's (1984) criteria, these inclusions can be considered primary. In other cases, they occur along secondary and/or pseudosecondary trails. Type I may coexists with type III inclusions in groups, in this case some inclusions of both types show variable liquid-to-vapour ratios.

Microthermometric measurements show that type I inclusions are characterized by Tmi between –6.7 and –1.6°C. In some inclusions of B3BIS-2108 sample Te could be measured between -20°C and –35. Clathrate melted (in the presence of an aqueous liquid phase and a carbonic gas) between -1.7 and 11.3°C. Solid and/or liquid CO_2 were not observed in these inclusions during freezing runs. Th ranged from about 170 and 335°C. Raman analyses indicated that the gas phase is largely made up of CO_2 (88-100 mole%), although significant amounts of CH_4 (up to 11 mole %) and less amounts of N2 (<4 mole %) are also present.

Table 1. Summary of the microthermometric results of type I inclusions. Abbreviations: P.d.T.=present-day temperature min.=host minerals, (l)=homogenization to the liquid phase, Q=quartz.

Sample	P.d.T. (°C)	M	Tmi (°C)	Tmcl (°C)	Th (°C)
B3BIS-2108	210	Q	-6.0/-2.8	6.0/9.6	199/276 (l)
B3BIS-3111	295	Q	-2.3/-1.6	6.7/11.3	276/302 (l)
B13BIS-3220	280	Q	-2.5/-1.8	3.0/10.0	306/336 (l)
B23-2036	195	Q	-3.8/-3.4	-1.7/-0.3	169/186 (l)

Type II, two-phase (liquid water + carbonic gas) liquid-rich inclusions show no clathrate formation during freezing. These inclusions are found along secondary and/or pseudosecondary trails within the B3BIS-31111 and B23-2036 samples in hydrothermal quartz and in B13BIS-3200 sample in hydrothermal calcite, while in the B22-2300 sample type II inclusions are hosted in hydrothermal quartz and adularia and may also show primary features (isolated inclusions), according to Roedder's (1984) criteria. In the PC33A-1690 these inclusions are hosted in metamorphic quartz along secondary trails and they are characterised by the widespread occurrence of a solid phase, which does not dissolve upon heating.

Tmi and Th of type II inclusions are rather variable ranging from –15.3°C to –0.8°C, and from about 150 to 325°C respectively . Te could be only measured in the B23-2036 sample and ranged between -48 and -38°C. Raman analyses indicated that CO_2 (95-100 mole%) is present in the bubble of the type II inclusions while CH4 (0-5 mole%) is present in small amount.

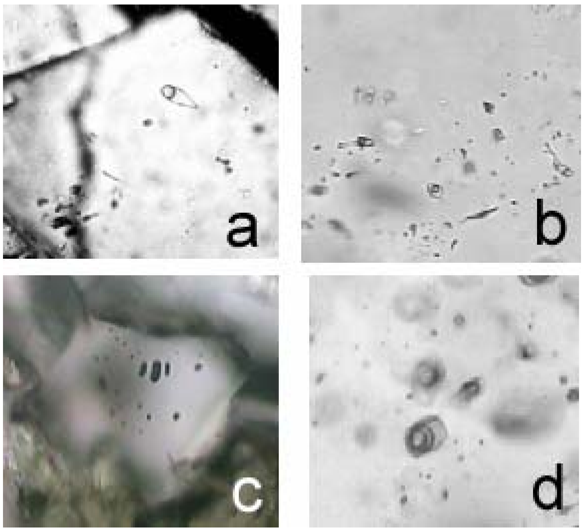

Figure 2: Microphotographs of the different fluid inclusion types found in the studied breccias: a) type I inclusions in quartz (B3BIS-3111), b) type II inclusions in quartz (Bg22-2300), c) type III inclusion in quartz (B13BIS-3200), d) type IV inclusions in quartz (PC33A-1690).

Table 2. Summary of the microthermometric results of type II inclusions. Abbreviations: same as in Table 1 and Cc=calcite.

Sample	P.d.T. (°C)	M	Tmi (°C)	Th (°C)
B3BIS-3111	295	Q	-1.6/-1.2	277/300 (l)
B13BIS-3220	280	Cc	-2.3/-1.8	227/275 (l)
B22-2300	320	Q	-1.2/-0.8	310/326 (l)
B23-2036	195	Q	-15.3/-13.8	152/161 (l)
PC33A-1690	205	Q	-15.0/-1.0	250/304 (l)

Type III, three-phase (carbonic gas + carbonic liquid + liquid water) or two-phase (carbonic gas + liquid water) volatile-rich inclusions or one-phase (carbonic gas) inclusions. These inclusions usually show variable liquid-to-vapour ratios and are present in all samples (hosted in quartz) with the exception of B22-2300 and B23-2036. In B13bis-3220 they occur in both hydrothermal quartz and calcite. These inclusions occur as three-dimensional groups of primary inclusions, often coexisting with type I inclusions, or along pseudosecondary and secondary trails. Raman analyses indicates that the volatile phase in type III inclusions consists mainly of CO_2 (94-100 mole %), with minor amount of CH_4 (0-6 mole %).

Table 3. Summary of the microthermometric results of type III inclusions. Abbreviations: same as in Table 1 and 2, and (v)=homogenization to the vapour phase, n.o.=not observed.

Sample	P.d.T. (°C)	M	TmCO2 (°C)	Tmi (°C)	Tmcl (°C)	ThCO2 (°C)	Th (°C)
B3BIS-2108	210	Q	-56.7/-56.3	-3.3/ -3.2	9.7/ 9.9	4.0/4.2 (v)	199/ 224 (v)
B3BIS-3111	295	Q	n.o.	n.o.	5.1/ 10.9	20.9/ 24.1 (l)	283/ 332 (v)
B13BIS-3220	280	Q	-56.9/-56.5	n.o.	7.6/ 9.8	2.5/8.8 (v)	301/ 326 (v)
B13BIS-3220	280	Cc	n.o.	n.o.	9.0/ 9.2	2.9/8.2 (v)	319 (v)
PC33A-1690	203	Q	n.o.	n.o.	9.1/ 9.5	n.o.	273 (v)

Type IV, three-phase (carbonic gas + carbonic liquid + liquid water) inclusions. These inclusions are considered to be trapped during a metamorphic event before the geothermal activity. In fact, these inclusions are always hosted in metamorphic quartz crystals along trails in the B3BIS-2108, B23-2036 and PC33A-1960 samples and their compositions (aqueous-carbonic fluid with a relatively dense carbonic phase) are typical of inclusions usually found in rocks interested by low to medium grade metamorphism (Roedder, 1984). This inclusions type is not of interest for the evolution of the geothermal fluids of the Mt. Amiata and therefore it will not be further discussed.

5. DISCUSSION

5.1 Fluid compositions

Table 4 reports the concentration ranges of CO_2, CH_4, N_2 (in mol/kg) and of the salinity (expressed as the sum of the concentrations of Na^+ and Cl^-) of the type I inclusions analysed by Raman, compared with the present-day values. Compositions of type I inclusions were computed using the "ICE" software of Bakker (1997), based on the Tmcl, Tmi, the composition of the gas phase determined by Raman micro-spectroscopy, and the volume fraction of the gas phase.

Table 4 also reports an approximate estimate of the salinity and CO_2 contents of type II inclusions. The CO_2 and CH_4 contents in the fluids of type II inclusions could not be precisely calculated since clathrate was not observed during freezing experiments. The absence of clathrate after final ice melting indicates only that the CO_2 content is <0.85 mol/kg (Hedenquist and Henley, 1985). The presence of CO_2 in type II inclusions, in addition, do not allow the exact determination of fluid salinity from Tmi, since the dissolved CO_2 in the aqueous phase contributes to ice melting depression up to 1.5°C (Hedenquist and Henley, 1985). The salinities of these inclusions computed from Tmi, using the equation of Bodnar and Vityck (1994), could be, therefore, overestimated up to 0.8 mol/kg.

The optical characteristics and rather variable liquid-to-vapor ratios of type III inclusions do not permit a reliable estimate of the volume fraction occupied by the gas phase; as a result the bulk compositions for such inclusions could not be computed.

Further information on the composition of the trapped fluid is given by Te. In particular, Te values, down to –35°C of some type I inclusions and down to –48°C for type II inclusions found in B23-2036 sample with low Tmi (-15.3/-13.8°C) indicate the presence of dissolved Ca^{2+} and/or Mg^{2+} in the fluid, in addition to Na^+, K^+ and Cl^-.

Table 4. Comparison between salinity, the CO_2, CH_4, N_2, concentration (in mol/kg) ranges of type I and II inclusions and the present-day geothermal fluid values. Fluid inclusions salinity is assumed to be equal to the sum of the Na^+ and Cl^- concentrations, salinity of present-day fluid equal to the sum of all the dissolved solids.

	Salinity (mol/kg)	CO_2 (mol/kg)	CH_4 (mol/kg)	N_2 (mol/kg)
Bagnore area				
Type I inclusions	0.11-2.24	1.27-2.68	0.00-0.09	0.00-0.04
Type II inclusions	0.20-4.00	<0.85	?	?
Present-day deep fluid	0.08-0.10	0.11-0.50	0.00-0.03	0.00-0.01
Piancastagnaio area				
Type II inclusions	0.30-3.90	<0.85	?	?
Present-day deep fluid	0.14	0.05	0.00	0.00

Table 4 shows that the trapped inclusions are characterized by wide salinity and CO_2 ranges. Comparison between present-day fluids and the trapped fluids indicates that type I inclusions salinity is higher than those of the modern fluid, although the lowest value in fluid inclusions nearly approaches present-day fluids value. The apparent salinities of type II inclusions (computed from the Tmi) could be overestimated (up to 0.8 mol/kg), therefore some of the trapped fluids, showing an apparent salinity of 0.2-0.9 mol/kg, might be actually have a salinity similar to the present-day fluids values (around 0.1 mol/kg). On the other hand, there are also type II inclusions with salinity higher then 0.9 mol/kg, indicating that a saline fluid circulated before present-day activity.

Table 4 also indicated that the CO_2 content of the fluids have undergone significant variation as suggested by the large range of CO_2 content in type I inclusions and by the significant difference between the CO_2 amount in type I and II inclusions.

5.2 Evidence of mixing and boiling processes

The diagram of Fig. 2 reports the Th vs. Tmi values of type I and II inclusions of Bagnore samples. Two main groups of data can be distinguished in this diagram: the first comprises most of the fluid inclusions and it is characterized by Tmi between –0.8 and -6.0°C, and Th between 169 and 336°C, the second is represented only by type II inclusions in BG23-2036 and is characterized by relatively low Tmi, between –15.3 and –13.8°, and Th, between 152 and 161°C. In the first group, the fluid inclusions with higher Th (275-335°C) show relatively low Tmi (from –2.3 to -0.8°C), whereas the inclusions with lower Th (170-275°C) usually display lower Tmi (from -6.0 to –2.0°C).

Since Tmi depends on the salinity (and in part on the CO_2 content) and Th is usually equal or close to the trapping temperature in geothermal systems (see also section 5.3), Tmi/Th variation can be in first approximation related to salinity/temperature changes. In hydrothermal systems, these changes can be in general due to by adiabatic boiling and/or fluid mixing processes (Hedenquist and Henley, 1985). Adiabatic boiling with steam loss would produce a salinity enrichment of about 100% considering a decrease of temperature, from 335 to 170°C (corresponding to the range of Th found in studied inclusions) due to the boiling process. These salinity increase, however, it is not sufficient to explain the high salinity variation shown in Table 4. The tendency shown in Fig 2 could be, therefore, imputed to a mixing process between two different types of fluids: a hot and low-salinity (i.e. low Tmi) fluid and a saline fluid of lower temperature. The latter fluid may be represented by the high-salinity, low-Th type II inclusions trapped in the B23-2036 sample.

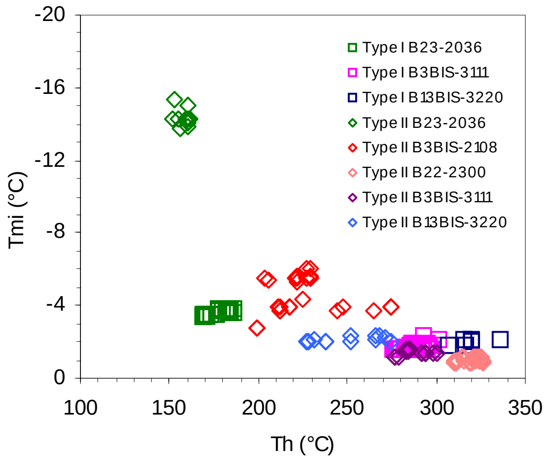

Figure 3: Th (total homogenization temperature) vs. Tmi (final ice melting temperature) diagram of type I and II inclusions of the Bagnore area.

A mixing process between fluids of different salinities but with roughly similar temperatures may be also hypothized for the fluid inclusions of PC33A-1690 samples on the basis of the Th/Tmi data (Fig. 3).

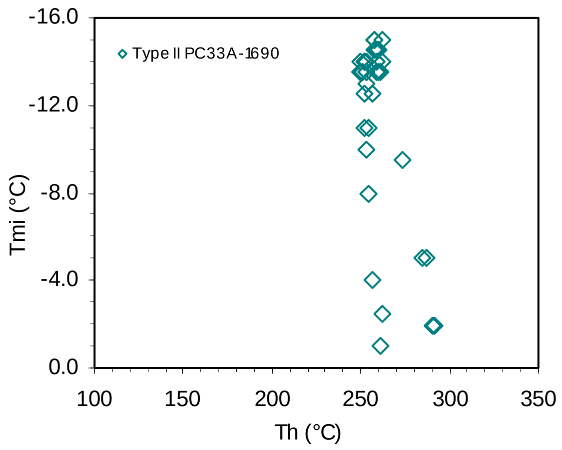

Figure 4: Th (total homogenization temperature) vs. Tmi (final ice melting temperature) diagram of type II inclusions of the Piancastagnaio area.

Fluid inclusions studies also suggest that boiling phenomena occurred during inclusions trapping. In particular, boiling is indicated in some samples (B3BIS-3111 and B13BIS-3220) by the coexistence of vapor-rich (type III) and liquid-rich (type I) inclusions or by the presence in the same crystal of primary type I and III inclusions: type III inclusions recording the aqueous-carbonic vapor produced by boiling and type I inclusions representing the boiling liquid.

If type I and III inclusions were both trapped during boiling, they should homogenize at the same temperature. In B13BIS-3220, since type I and III inclusions have similar Th ranges (Table 1 and 3) this condition is respected. In B3BIS-3111, type III inclusions display scattered Th values, this could be the result of heterogeneous (liquid+vapor) trapping. One consequence of this process is that the inclusions that trapped two phases have anomalously high Th with respect to the inclusions that trapped a single phase. Type III inclusions that may have trapped only the vapor phase are therefore the inclusions with lowest Th. In BG3BIIS-3111 the lowest Th values (283 and 289°C) of type III inclusions fall within the Th range (276-302°C) displayed by type I inclusions, supporting their trapping under boiling conditions.

In addition to fluid inclusions, also mineralogical data, such as the occurrence of calcite with bladed habit and adularia provide indirect evidence of boiling during the formation of hydrothermal minerals (Browne and Ellis, 1970; Keith and Muffler, 1978). In particular, these minerals were found in B3BIS-3111 and B13BIS-3220 samples, where boiling processes is also suggested by fluid inclusions, and also in BG22-2300 sample.

In B3BIS-2108 and PC33A-1690, type III inclusions also occur but they do not clearly coexist with type I or II inclusions. In this case, the trapping of type III inclusions only indicate that boiling processes took place somewhere in the system.

Boiling and/or mixing with a degassed liquid can also explain the wide CO_2 variation recorded by fluid inclusions and the decrease of the CO_2 content from fluid inclusion trapping towards present-day values.

In particular, in B3BIS-3111 and B13BIS-3220 samples the primary nature of many type I inclusions suggests that they record the early fluid circulation. On the other hand, type II inclusions are usually secondary in these samples and representing a late trapping event. The early fluid may have been trapped under boiling conditions as suggested by the coexistence of type I and III inclusions with similar Th. This fluid was characterized by high CO_2 content while in the late fluids, recorded in type II inclusions, the CO_2 concentration was lower (Table 4). The decrease of the CO_2 contents can be interpreted in terms of boiling processes. Since volatile components (CO_2, CH_4, N_2, etc.) strongly partition into the vapor phase, boiling and steam loss greatly deplete the liquid of these components (Hedenquist and Henley, 1985). Type II inclusions, therefore, probably record the most degassed fluid with CO_2 concentrations decreasing towards the present-day fluids values.

5.3 Fluid temperature

The Th of fluid inclusions usually corresponds to the minimum trapping temperature and it is equal to the trapping temperature only if inclusion trapping occurred under boiling condition (Roedder, 1984). In the studied samples the boiling phenomena at the sampling site is suggested only for B3BIS-3111, B13BIS-3220 and BG22-2300 samples. In the other samples, however, the difference between Th and the trapping temperature is usually small (<10°C considering hydrostatic pressure condition during fluid trapping) and the Th can be, therefore, considered nearly representative of the trapping temperature also in this samples.

From the comparison between present-day temperature and the fluid inclusions Th it can be noted that the samples with the highest present-day temperatures (B13BIS-3111 and B22-2300) have a limited Th ranges (≤26°C) of type I and II inclusions and that present-day temperatures are within these ranges. On the other hand, the other samples shows wide Th ranges for type I and II inclusions and the present-day temperatures are significantly lower (50-100°C) than the maximum Th recorded in B3BIS-2108, B13BIS-3220 and PC33A-1690 or slightly higher than the than the maximum Th recorded in B23-2036 sample.

This behaviour can be related to different thermal regimes in distinct part of the fields: the hottest areas (B13BIS-3111 and B22-2300) have been characterized only by small temperature variations from the time of fluid inclusions trapping. These variations may be due to limited boiling and/or mixing processes. The areas where lower present-day temperatures occur have been subjected by significant temperature changes. These changes may be explained with the sporadic infiltration of relatively saline and cold fluids (such as those recorded in the B23-2036 sample) that mixed with hotter and relatively low-salinity geothermal fluids. These saline fluid may be meteoric waters that infiltrated at depth and reacted with the evaporite layers present in the upper levels, within the “Tuscan Nappe”, of the stratigraphic sequence.

6. CONCLUSIONS

Fluid inclusions trapped in quartz, adularia and calcite found in core-sample drilled in wells of Bagnore and Piacastagnaio geothermal fields evidenced some changes of the some physical-chemical characteristics of the fluids that circulated present before present-day. In particular, a significant CO_2 decrease content in the fluid during inclusion trapping and than to present-day were imputed to boiling process with steam loss. Boiling processes are indicated by the coexistence of liquid-rich (type I) and vapor-rich (type III) inclusions and by mineralogical evidences, such as the occurrence of platy calcite and adularia.

Fluid inclusions also show large temperature/salinity variations that are can be related either boiling and to mixing processes. A mixing process between a hot low-salinity fluid and a cooler saline fluid probably occurred where present-day temperatures are not very high. Whereas in the hottest areas mixing processes did not apparently occurred and temperatures were not affected by significant changes.

ACKNOWLEDGMENTS

This work was partially supported by the COFIN2000 CROP18 project. The authors would like to thank ENEL GreenPower S.p.a. for providing the core samples and field data. Raman analyses in Siena have been provided by P.N.R.A.

REFERENCES

Baldi, P., Bellani, S. , Ceccarelli, A., Fiordelisi, A., Rocchi, G., Squarci, P., and Taffi L.: Geothermal anomalies and structural features of southern Tuscany (Italy), *Proceedings*, World Geothermal Congress, Florence, Italy (1995), 1287-1291.

Bakker, R.J.: Clathrates: computer programs to calculate fluid inclusions V-X properties using clathrate melting temperatures, *Computer and Geosciences*, **23**, (1997), 1-18.

Belkin, H., De Vivo, B., Gianelli, G. and Lattanzi, P.: Fluid inclusions in minerals from the geothermal fields of Tuscany, Italy, *Geothermics*, **14**, (1985), 59-72.

Bernabini, M., Bertini, G., Cameli, G.M., Dini, I., and Orlando, L.: Gravity interpretation of the Mt. Amiata geothermal area (central Italy), *Proceedings*, World Geothermal Congress, Florence, Italy, (1995) 859-862.

Bertini, G., Cappetti, G., Dini, I., and Lovari, F.: Deep drilling results and updating of geothermal knowledge of the Monte Amiata area, *Proceedings*, World Geothermal Congress, Florence, Italy (1995), 1283-1286.

Bodnar, R.J., and Vityk, M.O.: Interpretation of microthermometric data for H_2O-NaCl fluid inclusions. *De Vivo, B., Frezzotti, M.L.* (Eds.) Fluid inclusions in minerals: methods and applications. Short course of the working group (IMA) “Inclusions in Minerals” (1994), 117-130.

Browne, P.R.L., and Ellis, A.J.: The Ohaki-Broadlands hydrothermal area, New Zealand: mineralogy and related geochemistry, *American Journal of Science*, **269**, (1970), 97-131.

Cappetti, G., Passaleva G., and Sabatelli, F.: Italy country update report 1995-1999. *Proceedings*, World Geothermal Congress, Kyushu– Tohoku, Japan, (2000), 109-116.

Cathelineau, M., and Marignac, Ch.: Use of fluid inclusions for a better understanding of intracontinental geothermal activities, *De Vivo B., Frezzotti M.L.* (Eds.), Fluid inclusions in minerals: methods and applications. Short course of the working group (IMA) “Inclusions in Minerals” (1994), 309-326.

Ferrari, L., Conticelli, S., Burlamacchi L., and Manetti, P.: Volcanological evolution of the Monte Amiata, southern Tuscany: new geological and petrochemical data, *Acta Vulcanologica*, **8**, (1996), 41-56.

Fiordelisi A., Manzella, A., Buonasorte, G., Larsen, J., and Mackie, R.: MT methodology in the detection of deep, water-dominated geothermal systems, *Proceedings*, World Geothermal Congress, Kyushu-Tohoku, Japan (2000), 1121-1126.

Gianelli, G., Puxeddu, M. , Batini, F., Bertini, G., Dini, I., Pandeli, E., and Nicolich R.: Geological model of a young volcano-plutonic system: the geothermal region of Monte Amiata (Tuscany, Italy) *Geothermics*, 17, (1988), 719-734.

Hedenquist, J.W., and Henley, R.W.: The importance of CO_2 on freezing point measurements of fluid inclusions: evidence from active geothermal systems and implication for epithermal ore deposition, *Economic Geology*, **80**, (1985), 1379-1406.

Hedenquist, J.W., Reyes, A.G., Simmons, S.F., and Taguchi, S.: The thermal and geochemical structure of geothermal and epithermal systems: a framework for interpreting fluid inclusion data, *European Journal of Mineralogy*, **5**, (1992), 989-1016.

Keith, T.E.C., and Muffler, L.J.P.: Minerals produced during cooling and hydrothermal alteration of ash flow tuff from Yellowstone drill hole Y-5, *Journal of Volcanology and Geothermal Research*, **3**, (1978), 373-402.

Roedder, E.: Fluid inclusions, Mineralogical Society of America, *Reviews in Mineralogy,* **12**, (1984).